

Water Content in an Engineered Dermal Replacement during Permeation of Me₂SO Solutions Using Rapid MR Imaging

Nicolas P. Bidault,^{†,‡,§} Bruce E. Hammer,^{†,‡} and Allison Hubel^{*,†}

Departments of Biomedical Engineering and Radiology, CIA-MR, University of Minnesota, 420 Delaware Street SE, Mayo Mail Code 292, Minneapolis, Minnesota 55455, and Proctor & Gamble Rome Technical Center, via della Magliana 651, 00 166 Rome, Italy

The successful cryopreservation of cell and tissues typically requires the use of specialized solutions containing cryoprotective agents. At room temperature, the introduction of a cryopreservation solution can result in cell damage/death resulting from osmotic stresses and/or biochemical toxicity of the solution. For tissues, the permeation and equilibration of a cryoprotective solution throughout the tissue is important in enhancing the uniformity and consistency of the postthaw viability of the tissue. Magnetic resonance (MR) is a common nondestructive technique that can be used to quantitate the temporal and spatial composition of water and cryoprotective agents in a three-dimensional system. We have applied a recently developed rapid NMR imaging technique to quantify the transport of water in an artificial dermal replacement upon permeation of dimethyl sulfoxide (Me₂SO) solutions. Results indicate that the rate of water transport is slower in the presence of Me₂SO molecules. Furthermore, the transport is concentration-dependent, suggesting that Me₂SO tends to retain bound water molecules in the tissue. Moreover, water transport decreases with decreasing temperature, and the presence of cells tends to increase water transport.

Introduction

The prevalence of wounds to the skin has led to the development of various approaches to enhancing wound healing in the epidermis/dermis. Both a combined epidermal/dermal replacement sold under the name of Apligraf (1) and a dermal replacement sold under the name Dermagraft or TransCyte (2, 3) have been approved for use in the United States for the treatment of ulcers or burn wounds. These products have been some of the first engineered tissues to become commercially available for the treatment of tissue deficiencies. A wide variety of engineered tissues are in different stages of development.

The ability to cryopreserve engineered tissues is important for the clinical application of cell-based therapies. Specifically, cryopreservation permits the pooling of cells from different donors. Typically, the processing of these tissues is performed in specialized facilities usually associated with major research hospitals or biotechnology companies. The ability to store and transport engineered tissues will permit physicians and patients in rural areas or even foreign countries to benefit without traveling from their community. Cryopreservation also permits time for the completion of safety and quality control testing prior to use of the product in patients. The process of manufacturing an engineered tissue may require days to weeks for completion of the protocol. The ability to

cryopreserve the engineered tissues facilitates coordination of the therapy with patient care regimes.

The cryopreservation of cells and tissues had typically required the use of specialized solutions containing cryoprotective agents (CPAs). The addition of a CPA to the freezing solution may result in damage if it is not done properly. Specifically, the addition of a solute changes the tonicity of the solution. When exposed to high extracellular osmolarity, there is a rapid exoosmosis of water leaving the tissue followed by a slow incorporation of the penetrating CPA (due to its lower permeability). The volumetric excursions resulting from the fluxes of water and CPA can result in damage to the cells. Tissues and intact organs can exhibit reduced cellular viability when exposed to sufficiently large step changes in external osmolarity resulting from introduction or removal of a cryopreservation solution (4). Typically, solutions containing CPAs are introduced and removed using stepwise increments of increasing concentration in order to avoid the osmotic shock associated with single-step introduction or removal.

Not only are large step changes in osmolarity potentially damaging, but long-term exposure to even low concentrations of CPAs at room temperature can be lethal (5). Exposure of cells to CPAs (in particular Me₂SO) has been associated with a loss in viability with time of exposure. Subsequent studies have quantified specific cellular changes resulting from exposure to CPA, such as cytoskeletal reorganization, cross-linking of nuclear proteins, and alterations in membrane permeability (cf. ref 5 for review), which may account for the loss in viability. The toxicity of many CPAs has led to the development of protocols in which cryopreservation solutions are introduced at low temperature (4 °C) and the

* Ph: 612/626-2366. Email: hubel001@tc.umn.edu.

[†] Department of Biomedical Engineering, University of Minnesota.

[‡] Department of Radiology, University of Minnesota.

[§] Proctor & Gamble Rome Technical Center.

freezing protocol is initiated soon after introduction of the cryopreservation solutions. The reduction in temperature may suppress the kinetics of damage associated with exposure to the CPA, but it also suppresses the permeation of CPA into the tissue by increasing the time to equilibration.

Magnetic resonance (MR) is a common nondestructive technique used to quantitate the concentration of molecules inside 3D structures. Several MR techniques have been developed to quantitate the concentration of CPAs in tissues during permeation. Spectroscopic techniques have been used (6, 7); however, the information is not localized and concerns the entire tissue. Recently, investigators have used MRI to quantify the permeation of CPAs into biological systems. In one series of studies (8, 9), the permeation of dimethyl sulfoxide (Me_2SO), propylene glycol (PG), and methanol into zebra fish embryos was determined using a chemical shift imaging technique. Whereas these data were critical in confirming the role of the yolk syncytial layer as a barrier to CPA transport, the specific technique used suffers from limited temporal resolution. Isbell and colleagues (10, 11) measured the permeation of Me_2SO in rat kidney and liver tissue. Chemical shift specific slice selective (C4S) NMR imaging was used to determine the permeation of 50% w/w CPA solutions. The time per image was high (approximately 9 min), and the concentration of Me_2SO exceeds significantly the typical concentration used in the preservation of cells and tissues.

These studies point out the need for the use of NMR to image the permeation of CPAs into cells and tissues. These studies also illustrate the need to develop methods of imaging that are more practical (shorter imaging times and sensitivity to lower concentrations) and methods of quantifying and analyzing the data. Recently, a rapid imaging technique has been applied to the study of the permeation of CPA in artificial tissues (12). A combined FLASH-Keyhole technique was used to increase the speed and sensitivity of images obtained of CPA permeation in tissue. The technique enables to rapidly image the permeation of low concentrations of CPA. However, it suffers from possible image intensity distortions due to field inhomogeneity. Good field homogeneity across the field of view (FOV) is required to apply this imaging technique. The purpose of the present investigation is to visualize and quantify the transport of water in an engineered dermal replacement upon permeation of Me_2SO solutions using the aforementioned rapid imaging technique. The influence of CPA concentration, temperature, and presence of live cells on the water content of an engineered dermal replacement will be determined.

Materials and Methods

Culture of the Dermal Replacement. A collagen scaffolding was used to support the growth of the dermal fibroblasts and the formation of a dermal equivalent. Based on a protocol described in more detail by Doillon and colleagues (13), the scaffold consisted of 0.5% w/v collagen from bovine corium (Kensley-Nash, Exton, PA) mixed with 1:19 w/w % hyaluronic acid (Lifecore Biomedical, Inc., Chaska, MN) and dispersed in $\text{H}_2\text{O} + \text{HCl}$ solution at pH 3.0. The dispersion was frozen down to -30°C for 24 h and then freeze-dried for 48 h. The resulting collagen sponge was cross-linked in a vacuum oven for 5 days at 110°C .

Normal human dermal fibroblasts (Clonetics, Inc., San Diego, CA) were grown in a cell factory (Nunc, Inc., Naperville, IL) for 5 days with fibroblast culture medium

consisting of Dulbecco's Modified Eagles Medium (DMEM) (Gibco, Grand Island, NY) supplemented with 10% fetal bovine serum (FBS) (Hyclone, Logan, UT), 100 units/mL penicillin G, and 100 mg/mL streptomycin (Gibco). The harvested fibroblasts were seeded on the surface of the sponge at a density of 3×10^5 cells/cm². During culture of the fibroblasts in the collagen matrix, the fibroblast culture medium was supplemented with 10% w/w ascorbic acid (Gibco) every other day. The artificial dermis was cultured at 37°C and a 5% CO_2 atmosphere for 14 days with media changes every other day.

To evaluate the influence of the tissue matrix composition, with respect to the presence of cells and matrix proteins, some tissues were freeze-dried after being cultured. The freeze-drying step kills the cells infiltrated in the tissue, however, preserving intact the matrix proteins and cell debris.

Imaging Protocol. The imaging technique used in this investigation is based on a fast low-angle shot (FLASH) imaging sequence. The image acquisition is accelerated by a Keyhole acquisition mode for which only 32 phase encoding steps are recorded for each image instead of the 128 steps for a full k-space. A complete description of the NMR imaging technique can be found in ref 12.

For this investigation we are interested specifically in the transport of water in the engineered dermal replacement as a function of time. To discriminate between water protons present in the tissue from those present in the CPA solution (typically containing water, salts and CPAs), the external solution is replaced by a solution of $\text{Me}_2\text{SO} + 0.154 \text{ M NaCl} + \text{D}_2\text{O}$. Deuterium is invisible to NMR at the proton frequency, and this contrast will permit us to determine directly the transport of water during permeation with CPA solutions.

When D_2O is added to H_2O , there is an immediate equilibrium between the two compounds to give HOD, as follows: $\text{H}_2\text{O} + \text{D}_2\text{O} \rightarrow 2\text{HOD}$. The resonant frequency of HOD is the same as H_2O .

When the tissue is initially equilibrated with an isotonic saline solution (specifically, Hank's Balanced Salt Solution (HBSS) and the $\text{Me}_2\text{SO} + \text{NaCl} + \text{D}_2\text{O}$ solution is introduced around the tissue, only water protons from the tissue can be imaged. As D_2O molecules encounter H_2O molecules from the tissue, they react to form HOD molecules, which are NMR visible. Thus, the images obtained will show specifically the transport of water from the tissue. In a preliminary phase of this investigation, we mixed Me_2SO with D_2O and observed the proton spectrum for the mixture. No HOD molecules appeared in the mixture of Me_2SO and D_2O over several hours that the solution was monitored. Thus, no proton exchange between Me_2SO and D_2O was observed over the time of the permeation experiments, and therefore no dilution is expected from the presence of HOD molecules. Similar studies performed with other commonly used CPAs, specifically, glycerol and propylene glycol, did not yield similar results. $\text{D}_2\text{O} + \text{glycerol}$ or propylene glycol was observed to interact almost immediately to produce HOD, because the hydroxyl protons of glycerol and propylene glycol are free to exchange. For these two CPAs, water proton images will include both tissue water protons and HOD protons resulting from reaction of the CPA with D_2O . A more complete description of the basic physics behind this technique can be found in ref (18).

Permeation Experiments. Experimental Setup. To image the permeation of the CPA, the hydrated tissues (live or freeze-dried tissues) are cut in a band 7 mm wide and about 25 mm long to fit a custom plastic holder. The

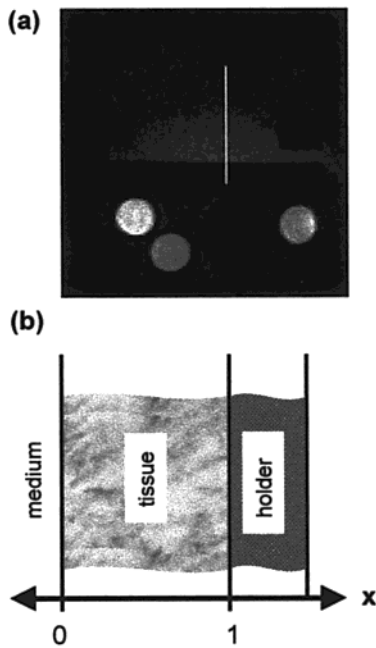


Figure 1. (a) FOV and permeation path. (b) Coordinate system for permeation path. The nominal thickness of the tissue is 1.5 mm.

sample holder is designed to limit the permeation of Me_2SO solutions to only one surface of the dermal replacement. After the tissue is secured into the holder, the holder and sample are introduced into an 8 mm i.d. glass tube (VWR, Chicago, IL) filled with HBSS. The sample is perfused with the cryopreservation system of interest. A more detailed description of the experimental setup can be found in ref 12.

The permeation characteristics of the solution can be influenced by temperature. For experiments performed at room temperature, no special control was performed, and the temperature inside the magnet was constant throughout the experiments ($19 \pm 1^\circ\text{C}$). For experiments at lower temperatures, tubing (i.d. 0.25 in.) was wrapped around the inner part of the shield. The tubing was connected to a temperature-controlled water bath (Fisher Scientific, Pittsburgh, PA). The temperature was monitored before and after the experiments by inserting a thermocouple inside the coil and reading the temperature on a thermocouple reader (Omega, Stamford, CT). Me_2SO solutions used in the low-temperature experiments were precooled in an ice bath prior to circulation.

Image Analysis and Data Quantification. Interpretation of the data obtained in this investigation requires the ability to specify the location and concentration of the water during the permeation experiments. The spatial location of the concentrations was determined along a permeation path. A permeation path defined on the image FOV, as well as the different regions of interest, is shown in Figure 1a and b. These regions include the medium, the tissue, and the sample holder, with the respective interfaces between these regions. The permeation path is chosen far away from the edges in order to avoid the contamination from the diffusion from the sides. The tissue-medium interface is defined by the interface between high and low intensity pixels on the first permeation image. Similarly, the interface between the tissue and the holder is determined from permeation images of fully permeated tissue. The x -axis along the permeation path is normalized to the thickness of the tissue, and $x = 0$ and $x = 1$ correspond, respectively, to

the interface tissue-sample holder and interface tissue-medium. The nominal thickness of the tissue was 1.5 mm.

Permeation Experiments and MRI Acquisition.

After the desired temperature was obtained in the coil prior to starting the permeation in the MR magnet, the magnetic field was shimmed to ensure optimal field homogeneity. A quick water image using the FLASH sequence was made to verify the uniformity of the sample in the slice. If inhomogeneities were observed in the slice (due to the presence of air bubbles or other large obstacles), the coil was removed from the magnet and the sample was repositioned. This process was repeated until good homogeneity in the slice was achieved.

At the beginning of the permeation experiment, the HBSS bathing solution was removed through the out port until no medium remained in the sample tube, and the outlet pump was turned off. The inlet pump was then turned on to introduce the $\text{Me}_2\text{SO}/\text{D}_2\text{O}$ solution. Once the $\text{Me}_2\text{SO}/\text{D}_2\text{O}$ solution filled the glass tube, the imaging experiment was started. Solutions of 10% and 50% v/v Me_2SO in D_2O were studied in both freeze-dried and live tissues.

All of the images have been obtained using the same MRI acquisition mode. All imaging was carried out on a 5.0 T 21-cm horizontal bore magnet (Magnex Scientific Limited, Oxon, UK) and Tecmag Libra (Tecmag, Houston, TX) imaging accessory. The imaging characteristics for water transport were as follows. The sweep-width was 3200 Hz, the in-plane gradient strength 2.25 G/cm, which conferred an in-plane resolution of $67 \mu\text{m}/\text{pixel}$ for a 128×128 image matrix. To avoid T_2^* weighting, the echo time, TE, was set to the minimum echo time achievable and was equal to 12.6 ms. The repetition time, TR, was chosen to minimize the imaging time and T1 weighting and was equal to 58 ms. Minimizing T1 weighting was also achieved by using a small flip angle of 10° . The FLASH RF pulse bandwidth was 3500 Hz. Four-step phase cycling was used on all images. To suppress the water signal after the CHESS pulse, crusher gradients of intensity 1.12 G/cm of x and y and 2.25 G/cm on z were applied for 1 ms. The slice thickness was set to the smallest thickness to produce images with reasonable S/N ratio and was equal to 2 mm. A maximum keyhole factor of 4 was obtained, and 32 phase encoding steps were used for the Keyhole images. At the end of the permeation image series, a full 128×128 image was obtained to reconstruct 128×128 images from the Keyhole images.

Water images in the presence of Me_2SO were made with the carrier frequency centered on the Me_2SO peak. For these images, 16 scans were used for a total imaging time of 40 s. Water images in absence of Me_2SO were made using the previous sequence deprived of the CHESS pulse. For these images, 16 scans were also used for a total imaging time of 20 s. The time between the introduction of the $\text{Me}_2\text{SO}/\text{D}_2\text{O}$ solution and the start of the imaging sequence was carefully measured using a chronometer. The origin of time, $t = 0$, corresponds to the introduction of the Me_2SO solution into the glass tube. Diffusion images were recorded until $t = 1.5$ h to allow full equilibration of the permeating solution.

Data Analysis. Dynamic Experiments. For each permeation image series, the water signal intensity is first converted to water concentration using three 1.5-mm diameter calibration tubes inserted in the FOV. These tubes contain a solution of 100% HBSS, 75% and 50% v/v HBSS in Me_2SO , which allow one to determine a calibration curve between water image intensity and

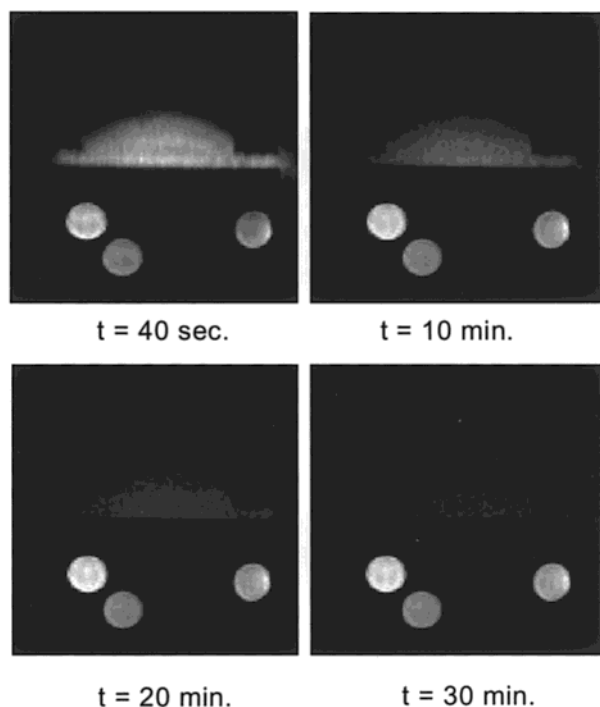


Figure 2. Permeation images at times from 40 s to 30 min for a 50% v/v Me₂SO in D₂O solution in a freeze-dried tissue at 19 °C. Light regions correspond to regions of high water concentration and dark regions high CPA solution concentrations.

water concentration for each permeation experiment. This calibration curve is then used to calibrate the water intensity in the tissue with water concentration. The water concentration is then normalized concentration of water at a given time and location divided by the initial concentration of water in the tissue prior to exposure to the CPA solution. The initial concentration of water was determined from the first permeation image using the region close to the sample holder in order to reduce the contamination with Me₂SO.

Results

Images obtained of the freeze-dried tissue upon permeation of a solution of 50% v/v Me₂SO in D₂O at 19 °C are shown in Figure 2. For short times, the freeze-dried tissue is light, indicating high water content. As time progresses, the tissue becomes darker, indicating permeation of the Me₂SO/D₂O solution. The position of the interface tissue-medium was monitored throughout the permeation images. With the spatial resolution of the images obtained, we did not observe any movement in the interface. This confirms that the thickness of the tissue is constant throughout the permeation within the spatial resolution of the images obtained.

A quantitative analysis of the concentration of water as a function thickness in the tissue and time can be obtained from the images obtained. The concentration of water is first normalized by dividing the image intensity at a given time and location by the intensity of water in the tissue at $t = 0$ (at a location close to the interface between the tissue and the wall of the holder). The three tubes of known composition present in the perfusion chamber are also used to establish a calibration curve to convert the intensities to concentrations. This type of analysis was used to quantify the water content with time in the tissue.

Water Transport Dynamics. Permeation of Me₂SO Solutions. We measured the normalized water concen-

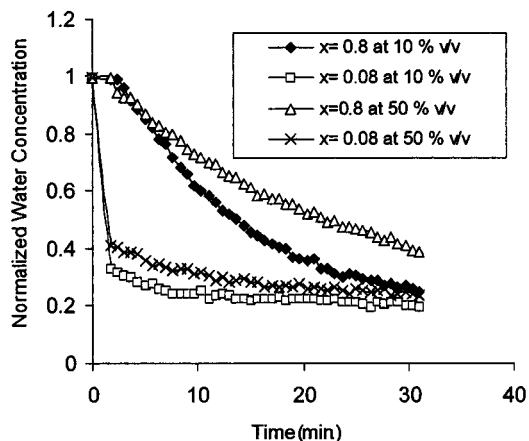


Figure 3. Normalized water concentration as a function of time for the freeze-dried tissue perfused with a cryoprotective solution at 19 °C. Solutions containing 10% and 50% v/v Me₂SO/D₂O were used.

tration as a function of time at two different locations in the engineered dermal replacement containing viable cells at room temperature upon the permeation of 10% and 50% v/v Me₂SO/D₂O solutions (Figure 3, see Figure 1 for coordinate system). As a control, we also performed a study characterizing the permeation of a pure D₂O solution in the same live dermal tissue at room temperature (Figure 3).

The normalized water concentration decreases as a function of time for all the locations and solution compositions tested. The final normalized water concentration for the tissue is approximately 25% in the presence of 10% Me₂SO, 30% in the presence of 50% Me₂SO and 15% in absence of Me₂SO. The final concentrations were calculated at $t = 1.5$ h, time at which complete equilibrium of the system is obtained (data not shown). The water equilibrium concentration increases with increasing Me₂SO concentration resulting from the strong interaction between water and Me₂SO molecules (see Discussion section). Because of concerns over the toxicity of cryoprotective solutions, the time for the tissue to equilibrate is an important parameter. For this investigation, the equilibration time was estimated to be the time at which the normalized water concentration for the given location reaches equilibrium. For a 10% Me₂SO solution, the time to equilibration at the region adjacent to the tissue-medium interface ($x = 0.08$) was approximately 7 min. At the edge of the tissue close to the sample holder, the equilibration time increased to approximately 30 min. For a higher concentration solution (50% Me₂SO), the equilibration time at $x = 0.08$ increased to 17 min. Thus, the permeation of the CPA solution decreases as the initial concentration of cryoprotectant increases. In absence of CPA (pure D₂O solution), the equilibrium at the interface tissue/medium ($x = 0.09$) is reached after approximately 7–10 min, which is equivalent to the equilibration time of the lower concentrated CPA solution (10% Me₂SO). Close to the sample holder ($x = 0.8$) the equilibration time is increased to approximately 22 min, which is shorter than that for the solution containing CPA. Thus, the results tend to indicate that the permeation of CPA solutions holds tissue water inside the tissue for longer time. With increasing concentration of CPA in the medium, the time to equilibration increases.

Influence of Viable Cells. The presence of viable cells may influence the water content and water concentration as a function of time in the engineered dermal replace-

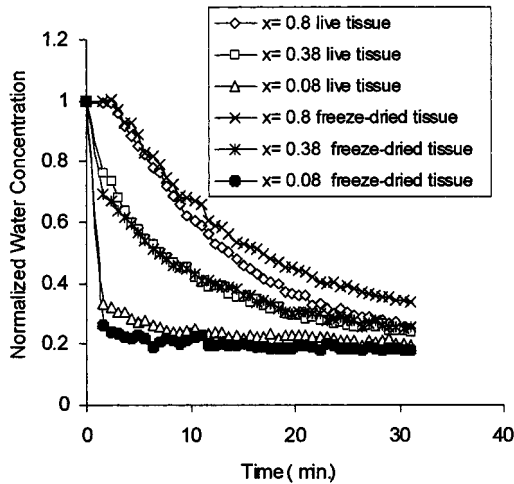


Figure 4. Normalized water concentration as a function of time for the freeze-dried dermal replacement and a dermal replacement containing viable cells. The samples were perfused with a solution containing 10% v/v $\text{Me}_2\text{SO}/\text{D}_2\text{O}$ solution at 19 °C.

ment. Cells infiltrate the artificial dermal replacement throughout the thickness of the tissue. The density of the cells is much higher on the edge (i.e., surface) of the tissue than inside the tissue (results not shown). The next phase of the investigation involved determining the water content as a function of time for the freeze-dried dermal replacement and a dermal replacement containing viable cells perfused with a CPA solution containing 10% Me_2SO (Figure 4).

At the solution/tissue interface ($x = 0.08$) for time less than 10 min, the normalized water content of the dermal replacement with viable cells is greater than that of the freeze-dried tissue. At $x = 0.38$, the differences in normalized water content between the two systems tested were present for only 2–3 min. At later time, the normalized water concentration in the two systems is identical. For $x = 0.8$, the normalized water content of the freeze-dried tissue is greater than that of the dermal replacement with viable cells for times greater than approximately 10 min. These results indicate that the presence of viable cells has an influence on the water content in an engineered tissue that varies with time and location. The higher concentration of cells at one surface of the dermal replacement did not result in any observable or quantifiable difference in signal intensity across the width of the tissue. Additional studies using different cell concentrations are needed to determine in more detail the influence of viable cells on water content as a function of spatial location and time.

Influence of the Temperature. As indicated previously, the introduction of CPA solutions is frequently performed at lower temperatures in order to minimize the toxicity of the solution. As such, the next phase of the investigation involved determining the water concentration as a function of time and temperature. The water concentration at two different locations in the freeze-dried tissue upon the permeation of 50% v/v $\text{Me}_2\text{SO}/\text{D}_2\text{O}$ solutions at 19 and 0 °C is shown in Figure 5.

The results indicate that the decrease in water concentration is slower at lower temperature throughout the tissue. For $x = 0.75$, the water concentration is the same at both temperatures for the first 2–3 min. This results from the fact that the permeating solution has not yet reached this region of the tissue (see Figure 3). At

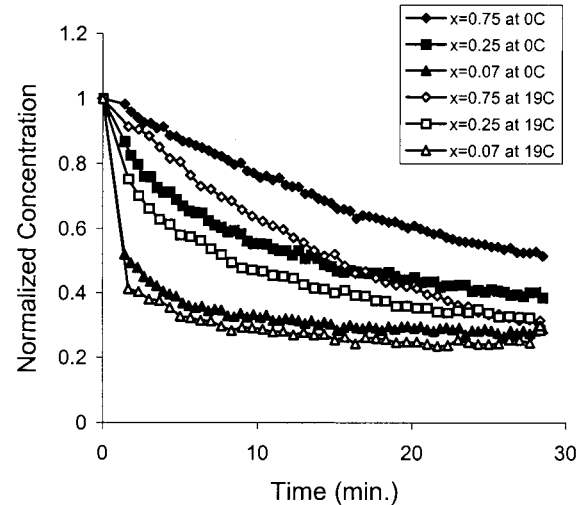


Figure 5. Normalized water concentration in different locations in a freeze-dried tissue upon permeation of a 50% v/v $\text{Me}_2\text{SO}/\text{D}_2\text{O}$ solution at 19 and 0 °C.

later times the normalized water concentration exhibits significant differences for the same location at 19 versus 0 °C.

Water Volume Profiles. Finally, in the last phase of the investigation, we determined the change of the total water volume of the tissue for the different conditions described previously. At time $t = 0$, the entire tissue has a uniform water content across its thickness, and the water concentration is 100% v/v. We assume that the thickness of the tissue is constant throughout the permeation of the $\text{Me}_2\text{SO}/\text{D}_2\text{O}$ solution. We will define the volume of water in the tissue, at time t , as the area under the graph of water concentration as a function of location. The relative volume of water in the tissue is then given by the ratio of the volume of water at time t and the initial volume of water. The variations of the tissue water volume for live tissue at 19 °C are given in Figure 6. A rapid efflux of water is observed at the tissue/solution interface during the first minute(s) of exposure to the CPA solution. At a time of 30 min, the water concentration across the thickness of the tissue is largely constant (20% v/v).

Discussion

Permeation of Me_2SO Solutions. The results of this investigation indicate that for the solutions studied, the addition of Me_2SO to the cryopreservation solution reduced the transport of water out of the tissue (see Figure 3). For this investigation, the equilibration time is defined as the time for which the concentration at a given location reaches 95% of its final value. The time to equilibration of the water content of the tissue varied between 30 and 40 min for 10% and 50% v/v Me_2SO solutions, respectively, for interior portions of the dermal replacement. For the same location using a D_2O solution without Me_2SO , the time to equilibration was considerably less (22 min). The reduction in water transport observed in this investigation is consistent with previous studies. The most likely reason for the change in water transport characteristics with increasing Me_2SO concentration may involve hydrogen bonding of the water molecules. At -20 °C, 1 mol of Me_2SO binds 3 mol of water (14). Moreover, it has been observed that proton bonds between water and Me_2SO molecules are 1.33 times stronger than those solely between water molecules (14). The transport of water and CPA in isolated cells

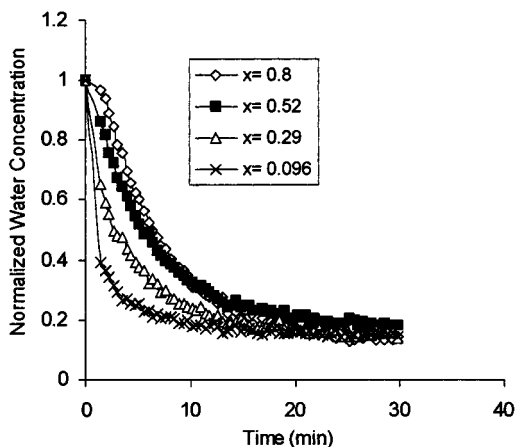


Figure 6. Normalized water volume as a function of time for a dermal replacement containing live cells exposed to a solution containing 10% v/v Me₂SO/D₂O solution at 19 °C.

has been analyzed previously by Kedem and Katchalsky (15):

$$\frac{dn_s}{dt} = -L_p(1 - \sigma)c_s^m ART\Delta c_i + [\omega - \sigma L_p(1 - \sigma)c_s^m]ART\Delta c_s$$

where n_s is the number of moles of CPA; L_p is the hydraulic permeability of the membrane; A is a constant that relates the melting temperature of the extracellular solution to its composition; v_w is the molar volume of water; σ and ω are the reflection coefficient and solute mobility coefficient, respectively; T is the temperature and Δc is the difference in concentration for water (i) and solute (s) across the membrane; c_s^m is the average solute concentration across the cell membrane. In their mathematical model, Kedem and Katchalsky introduced three phenomenological coefficients: L_p , ω , and σ . L_p is the hydraulic conductivity ($\mu\text{m}/\text{min}\cdot\text{atm}$); ω is the solute mobility ($\text{mol}/\text{N}\cdot\text{s}$); and σ is the reflection coefficient (no units). This mathematical model has been derived for transport in cells; however, it has also been applied to vascularized tissue (16). In that case, the phenomenological coefficients refer to permeability through the whole tissue. Shabana and McGrath have demonstrated that L_p is dependent on the solute concentration in isolated cells (17). Moreover, results from Figure 3 indicate that the equilibration water concentration is lower in absence of Me₂SO. The water concentration at equilibrium at both locations in the tissue is approximately 25% in the presence of 10% Me₂SO and 30% in the presence of 50% Me₂SO and approximately 15% in absence of Me₂SO. The NMR signal intensity is composed of the water signal coming from the molecules traveling during permeation and molecules that do not take part in the permeation and are bound to the matrix. At equilibrium, the tissue matrix and cells are fully equilibrated with the permeating solution (Me₂SO/D₂O). In absence of Me₂SO, the equilibrium water concentration is 15%. In presence of Me₂SO, the equilibrium water concentration is higher, indicating that the presence of Me₂SO retains water molecules in the tissue. Thus, the higher the Me₂SO concentration, the higher the water equilibrium concentration. Another possible influence for the observed changes in water transport characteristics with concentration may involve changes in the physical interactions between molecules with increasing Me₂SO concentration. Specifically, increasing Me₂SO concentration may result in increasing solution viscosity.

Influence of Viable Cells. The presence of viable cells in the tissue represents a potentially significant factor in the transport parameters. Specifically, if the cell density is high, the water content of the cells embedded in the matrix may be a significant fraction of the total water present. As we are looking at low molecular weight cryoprotective agents that can penetrate the cell membrane, the role of the cell membrane in the permeation and equilibration of a cryoprotective solution is also of interest. For the system used in this investigation, the presence of cells does not influence the equilibrium water concentration, as indicated in Figure 4. However, as seen in Figure 4, the presence of cells influences the water transport. Inside the tissue, where the density of cells is low (results not shown), the water concentration is identical independently of the presence of cells. However, close to the sample holder, on the edge of the tissue, the water concentration in the presence of cells is lower than in absence of cells after approximately 10 min. On the edge of the tissue, the concentration of cells is high. The permeating solution penetrates the tissue, resulting in an increase of the osmolarity of the extracellular solution. By osmosis, the cells dehydrate, resulting in an extra loss of water, with respect to that in the freeze-dried tissue.

The results at lower temperature (Figure 5) indicate that the transport at lower temperature is much slower than at room temperature. Classical cryopreservation protocols include permeating the CPA solution at lower temperature to reduce osmotic stresses and minimize biochemical toxicity of CPA solutions. The introduction of CPA solutions at lower temperatures will increase the time to equilibration, and CPA introduction protocols for tissues must be modified to reflect the differences in transport characteristics with temperature.

The results on the water transport in the tissue indicate a rapid efflux of water upon permeation of a Me₂SO/D₂O solution, which occurs within 1 min after introduction of the CPA solution. This rapid water efflux has already been reported by Walcerz et al. (6). They have studied the permeation of Me₂SO in cornea slices, using NMR spectroscopy. Using the Kedem–Katschalsky mathematical model to fit their data, they computed L_p , ω , and σ and generated data on water and Me₂SO transport in the tissue. They observed a rapid efflux of water during the first 1.5 min after exposure to the CPA solution at both 22 and 0 °C. Walcerz et al. also computed the change of corneal volume (total tissue volume) from the mathematical model. They defined a relative volume as calculated volume divided by volume under isotonic conditions and normal stromal hydration. They observed that exposure to 2.0 mol/L (13% v/v) Me₂SO produced an initial volume decrease during the first 1.5 min of exposure to the CPA solution of 32% at 22 °C and 31% at 0 °C. Our results (Figure 6) indicate a decrease of 30% of total water volume during the first minute of exposure to 10% v/v Me₂SO solution at 19 °C and of 20% for an exposure of 50% v/v Me₂SO solution at 0 °C. Our result at room temperature is consistent with that of Walcerz et al. However, at 0 °C they observed a larger decrease in tissue volume than we did at the same temperature in the artificial tissue. The differences in cell type and matrix composition between the two studies may play a significant role in the differences in behavior observed.

Conclusion

In this paper we have presented temporal and spatial quantitative data on the water transport in a cultured dermal equivalent upon permeation of Me₂SO solutions. This newly developed technique enables us to visualize

and quantify the transport in tissues. In the case of low-density artificial tissues, short imaging time is required. However, this technique still suffers from signal contamination from bound water molecules. True images of diffusing molecules could be obtained with other NMR techniques, such as magnetic resonance transfer, or diffusion weighted imaging. Moreover, this paper focused on water transport upon permeation of Me₂SO solutions. However, the technique should not be limited to that CPA, and a thorough understanding of the interaction of other molecules with D₂O could definitely reveal other CPA candidates for this technique.

References and Notes

- (1) Eaglestein, W. H.; Falanga, V. Tissue engineering and the development of Apligraf, a human skin equivalent. *Adv. Wound Care* **1998**, *11*, 1–8.
- (2) Bowering, C. K. Dermagraft in the treatment of diabetic foot ulcers. *J. Cutan. Med. Surg.* **1998**, *3 Suppl 1*, S1–29–32.
- (3) Noordenbos, J.; Dore, C.; Hansbrough, J. F. Safety and efficacy of TransCyte for the treatment of partial-thickness burns. *J. Burn Care Rehabil.* **1999**, *20*, 275–281.
- (4) Pegg, D. E. Perfusion of rabbit kidneys with cryoprotective agents. *Cryobiology* **1972**, *9*, 411–419.
- (5) Fahy, G. M.; Lilley, T. H.; Linsdell, H.; Douglas, M. S.; Meryman, H. T. Cryoprotectant toxicity and cryoprotectant toxicity reduction: in search of molecular mechanisms. *Cryobiology* **1990**, *27*, 247–268.
- (6) Walcerz, D. B.; Taylor, M. J.; Busza, A. L. Determination of the kinetics of permeation of dimethyl sulfoxide in isolated corneas. *Cell Biophys.* **1995**, *26*, 79–102.
- (7) Fuller, B. J.; Busza, A. L. Proton NMR studies on the permeation of tissue fragments by dimethyl sulphoxide: liver as a model for compact tissues. *Cryo-Lett.* **1994**, *15*, 131–134.
- (8) Hagedorn, M.; Hsu, E. W.; Pilatus, U.; Wildt, D. E.; Rall, W. R. et al. Magnetic resonance microscopy and spectroscopy reveal kinetics of cryoprotectant permeation in a multicompartmental biological system. *Proc. Natl. Acad. Sci. U.S.A.* **1996**, *93*, 7454–7459.
- (9) Hagedorn, M.; Hsu, E.; Kleinhans, F. W.; Wildt, D. E. New approaches for studying the permeability of fish embryos: toward successful cryopreservation. *Cryobiology* **1997**, *34*, 335–347.
- (10) Isbell, S. A.; Fyfe, C. A.; Ammons, R. L.; Pearson, B. Measurement of cryoprotective solvent penetration into intact organ tissues using high-field NMR microimaging. *Cryobiology* **1997**, *35*, 165–172.
- (11) Isbell, S. A. Development of a protocol for the quantitative evaluation of contrast in NMR images of cryoprotective solvents in intact tissues. *Cryobiology* **1997**, *34*, 165–175.
- (12) Bidault, N. P.; Hammer, B. E.; Hubel, A. Rapid MR imaging of cryoprotectant permeation in an engineered dermal replacement. *Cryobiology* **2000**, *40*, 13–26.
- (13) Doillon, C. J.; Whyne, C. F.; Brandwein, S.; Silver, F. H. Collagen-based wound dressings: control of the pore structure and morphology. *J. Biomed. Mater. Res.* **1986**, *20*, 1219–1228.
- (14) Karow, A. M. Biophysical and chemical considerations in cryopreservation. In *Organ Preservation for Transplantation*; Little, Brown: Boston, MA, 1974; p 124.
- (15) Kedem, O.; Katchalsky, A. Thermodynamic analysis of the permeability of biological membranes to nonelectrolytes. *Biochim. Biophys. Acta* **1958**, *27*, 229–246.
- (16) Rubinsky, B.; Cravalho, E. G. Transient mass transfer processes during the perfusion of a biological organ with a cryophylactic agent solution. *Cryobiology* **1982**, *19*, 70–82.
- (17) Shabana, M.; McGrath, J. J. Cryomicroscope investigation and thermodynamic modeling of the freezing of unfertilized hamster ova. *Cryobiology* **1988**, *25*, 338–354.
- (18) Jackman, L. M.; Cotton, F. A. *Dynamic NMR Spectroscopy*; Academic Press: New York, 1975.

Accepted for publication April 2, 2001.

BP010033Y